

Application of luminescent Eu:Gd₂O₃ nanoparticles to the visualization of protein micropatterns

Dosi Dosev

University of California Davis
Department of Mechanical and Aeronautical
Engineering
Davis, California 95616

Mikaela Nichkova

University of California Davis
Department of Entomology
Davis, California 95616

Maozi Liu

University of California Davis
Department of Chemistry
Davis, California 95616

Bing Guo

University of California Davis
Department of Mechanical and Aeronautical
Engineering
Davis, California 95616

Gang-yu Liu

University of California Davis
Department of Chemistry
Davis, California 95616

Bruce D. Hammock

University of California Davis
Department of Entomology
Davis, California 95616

Ian M. Kennedy

University of California Davis
Department of Mechanical and Aeronautical
Engineering
Davis, California 95616

1 Introduction

Lanthanide oxides are commonly used luminescent materials in the lighting industry.^{1,2} Nanoparticles of lanthanide oxides are also promising labels in biotechnology because of their optical properties, such as large Stokes shift, lack of photobleaching, and long luminescence lifetime (about 1 ms). The large Stokes shift enables the subtraction of the excitation wavelength by filtering, while the long lifetime enables time-gated detection and subtraction of the background autofluorescence. In addition, the synthesis of lanthanide oxides is

Abstract. Nanoparticle phosphors made of lanthanide oxides are a promising new class of tags in biochemistry because of their large Stokes shift, sharp emission spectra, long luminescence lifetime, and good photostability. We demonstrate the application of these nanoparticles to the visualization of protein micropatterns. Luminescent europium-doped gadolinium oxide (Eu:Gd₂O₃) nanoparticles are synthesized by spray pyrolysis. The size distribution is from 5 to 200 nm. The particles are characterized by means of laser-induced fluorescent spectroscopy and transmission electron microscopy (TEM). The main emission peak is at 612 nm. The nanoparticles are coated with avidin through physical adsorption. biotinylated bovine serum albumin (BSA-b) is patterned on a silicon wafer using a microcontact printing technique. The wafer is then incubated in a solution of avidin-coated nanoparticles. Fluorescent microscopic images reveal that the nanoparticles are organized onto designated area, as defined by the microcontact printing process. The luminescent nanoparticles do not suffer photobleaching during the observation, which demonstrates their suitability as luminescent labels for fluorescence microscopy studies. More detailed studies are performed using atomic-force microscopy (AFM) at a single nanoparticle level. The specific and the nonspecific binding densities of the particles are qualitatively evaluated. © 2005 Society of Photo-Optical Instrumentation Engineers. [DOI: 10.1117/1.2136347]

Keywords: nanoparticles; lanthanide; luminescence; biosensor; microcontact printing.

Paper 05082R received Mar. 24, 2005; revised manuscript received Aug. 19, 2005; accepted for publication Aug. 20, 2005; published online Nov. 18, 2005. Paper 05082R received Mar. 24, 2005; revised manuscript received Aug. 19, 2005; accepted for publication Aug. 20, 2005. This paper is a revision of a paper presented at the SPIE conference on Imaging, Manipulation, and Analysis of Biomolecules and Cells: Fundamentals and Applications III, Jan. 2005, San Jose, CA. The paper presented there appears (unrefereed) in SPIE Proceedings Vol. 5699.

quick, simple, and scalable for mass production. Particles with different emission spectra can be easily obtained by controlled doping of lanthanide ions into an appropriate host material.³ Host materials such as Gd₂O₃ or Y₂O₃ are ideal hosts for lanthanide; the lanthanide ions are located at sufficient distances from each other to avoid self-quenching. As a result, the doped materials have more efficient luminescence than pure lanthanide oxides³ (Eu₂O₃, Tb₂O₃). In contrast with semiconductor quantum dots,⁴ the emission wavelength of the lanthanide oxide nanoparticles is independent of the particle size, and a relatively broad size distribution can be tolerated in some applications. This enables us to work within a size range that is mainly determined by the particular application.

Address all correspondence to Ian Kennedy, Mechanical and Aeronautical Engineering, University of California/Davis, One Shields Avenue, Bainer Hall, Davis, California 95616; Tel: 1 530 752 2796; Fax: 1 530 210 8220; E-mail: imkennedy@ucdavis.edu.

These unique properties of the lanthanide oxide nanoparticles make them promising candidates for low-cost applications in biochemistry.

Although the useful properties of lanthanide oxides have been reported extensively in the literature, there are not many applications in biotechnology in contrast to the intensively studied quantum dots.⁵⁻⁷ Preliminary results using europium oxide (Eu₂O₃) nanoparticles as labels for environmental immunoassay have already been reported showing enhanced assay sensitivity.⁸

Emerging techniques in biochemistry and biosensor development are based on protein and DNA microarrays. Microarrays are usually visualized under fluorescent and/or confocal microscopes using organic fluorescent dyes.⁹ Dye photobleaching can significantly reduce the available time for observation; hence photostability of the fluorophores is of crucial importance for this type of application. In this paper, we optimized a method for coating Eu:Gd₂O₃ particles with proteins and demonstrate the use of these particles as phosphores for the visualization of protein micropatterns. Avidin-biotin specific binding was used as a model system.

2 Experiment

2.1 Chemicals and Materials

Europium(III) nitrate Eu(NO₃)₃·5H₂O and gadolinium(III) nitrate Gd(NO₃)₃·6H₂O were purchased from Sigma for the synthesis of luminescent Eu:Gd₂O₃. Polystyrene microspheres doped with Eu chelates were purchased from Seradyn Inc. Avidin and bovine serum albumin (BSA) were obtained from Sigma. Immunopure biotinylated BSA (BSA-b, 8 moles biotin/mol protein) was purchased from Pierce. The 5-carboxyrhodamine 6G, succinimidyl ester was obtained from Sigma. Avidin-rhodamine 6G was prepared by a conjugation reaction between the amine groups of the protein and the succinimidyl ester of the 5-carboxyrhodamine 6G following a standard procedure recommended by Molecular Probes.¹⁰ The degree of labeling obtained was 2 moles rhodamine/mol avidin. Deionized water (18 MΩ cm) was obtained using a Millipore purification system. Phosphate buffered saline (PBS) (pH 7.5) was 10-mM phosphate buffer, 0.8% saline. Black 96-well plates from Nunc were used for fluorescence measurements. The polydimethylsiloxane (PDMS) stamp used in microcontact printing had a linewidth of 5 μm. An *n*-doped Si wafer was used as a substrate for microcontact printing and atomic force microscopy (AFM) characterization.

2.2 Instrumentation

The size and the shape of the Eu:Gd₂O₃ nanoparticles were determined using a Philips CM-12 transmission electron microscope (TEM). An Opolette™ tunable pulsed optical parametric oscillator (OPO) laser (Opotek, California) was used for fluorescence excitation of the nanoparticles and their luminescence spectra were recorded using a Spectra Pro 300i gated intensified spectrometer (Princeton Instruments Inc). A Spectramax M2 microplate reader (Molecular Devices, Sunnyvale, California) was used for the detection of rhodamine fluorescence. An ultrasonic bath 75D (VWR) was used for treating the nanoparticle suspensions and for cleaning

procedures. The centrifuges used for nanoparticle sizing were a Sorvall® RC5B Plus Centrifuge (Kendro Laboratory Products) and a Centrifuge 5415D (Eppendorf).

Fluorescence images were obtained by an epifluorescent microscope (Nikon Microphot-SA) equipped with a 400-nm dichroic mirror cube (DM 400) and a 100-W mercury lamp. A computer-controlled CCD camera RT Color, model 2.2.1 from Diagnostic Instruments Inc. was coupled to the fluorescent microscope and was used for digital visualization of the fluorescent images. A dichroic cube with a threshold wavelength of 400 nm was used to separate the UV excitation ($\lambda_{\text{ex}} < 400$ nm) from the visible luminescent emission ($\lambda_{\text{em}} > 400$ nm). The CCD camera, image capture, and analysis were controlled by "Spot" software.

The AFM used for this work is a MFP-3D (Asylum Research, Santa Barbara, California). The ultrasharpened Si₃N₄ AFM tip was obtained from Veeco (Santa Barbara, California) with a spring constant of 0.1 nN m⁻¹. The AFM images were obtained using the contact mode at a scan speed of 1 to 2 Hz. The image force was under 5 nN. The topography and lateral force images were taken in air at room temperature.

2.3 Synthesis of Eu:Gd₂O₃ Nanoparticles

Luminescent Eu:Gd₂O₃ nanoparticles were synthesized by a spray pyrolysis method that is described in detail elsewhere.¹¹ Briefly, an ethanol solution containing 20-mM Eu(NO₃)₃ and 80-mM Gd(NO₃)₃ was sprayed into a hydrogen diffusion flame through a nebulizer. The flame was formed by an H₂ flow at 2 L min⁻¹ and an air coflow at 10 L min⁻¹, surrounding the outlet of the nebulizer. A flame temperature above 2100°C was reached. Oxidation reactions took place within the flame to form Eu:Gd₂O₃ nanoparticles. A cold finger was used to collect the Eu:Gd₂O₃ particles thermophoretically. The production rate of this synthesis procedure was about 400 to 500 mg h⁻¹. The as-synthesized particles were suspended in methanol in an ultrasonic bath for 30 min to break any weak agglomerates formed during the collection process. Particles larger than 200 nm in diameter were settled from the primary suspension by means of selective centrifugation at 1000×*g* for 2 min. The nanoparticles from the supernatant (diameter below 200 nm) were extracted and dried for subsequent use.

2.4 Coating of Eu:Gd₂O₃ Nanoparticles with Avidin

Eu:Gd₂O₃ nanoparticles (1 mg) were suspended using an ultrasonic bath in 1 ml of 25-mM carbonate-bicarbonate buffer, pH 8.6, in a polypropylene tube, previously coated with 0.5% BSA to avoid loss of avidin to the tube walls. A solution of 2 mg ml⁻¹ avidin (100 μl) was added to the particle suspension and incubated in a rotating mill overnight at room temperature. The suspension was then centrifuged at 15,000×*g* for 3 min. The supernatant was discarded and the nanoparticle pellet was resuspended in the same buffer to wash off the excess protein. This washing procedure was repeated 3 times. To ensure that no bare particle surface remained, the avidin-Eu:Gd₂O₃ nanoparticles were incubated in 1 ml of 0.5 mg ml⁻¹ BSA solution in 25-mM phosphate buffer for 1 h at room temperature in the rotating mill. After three con-

secutive washings by centrifugation and resuspension, the avidin-Eu:Gd₂O₃ nanoparticles were used for the microplate detection assays.

The surface saturation capacity of the nanoparticles with respect to avidin was evaluated following the same coating procedure, using avidin-rhodamine complex instead of avidin. After efficient washing of the excess avidin-rhodamine from the coating solution, the nanoparticle pellet was resuspended in 100 μ l of carbonate-bicarbonate buffer. The fluorescence of rhodamine (excitation, 520 nm; emission, 550 nm) adsorbed on the particle surface was measured on the microplate reader and was used as an indication for the amount of adsorbed avidin molecules.

An identical coating with neutravidin rather than with avidin produced a smaller amount of protein adsorbed to the nanoparticle's surface. This result strongly suggests that the higher positive charge of hen egg avidin (isoelectric point PI=10.0), compared to that of neutravidin (PI=6.3), contributes to the stronger adsorption to the negatively charged particle surface. This observation is consistent with other studies on protein adsorption onto quantum dots based on electrostatic interactions.¹²

2.5 Microcontact Printing of Biotinylated BSA: Substrate, Stamp, and Sample Preparation

A silicon (100) wafer was used as a solid substrate for microcontact printing of proteins and the consecutive specific interactions. Prior to use, the silicon wafer was thoroughly washed in an ultrasound bath in acetone, ethanol, and deionized water for 10 min each. Finally, it was dried under a nitrogen stream. The PDMS stamp was washed by sonication in ethanol (3 \times 10 min), dried under nitrogen and exposed to the solution of the inking protein (50 μ g ml⁻¹ BSA-b in PBS) for 40 min. Excess solution was removed and the stamp was dried under a stream of nitrogen gas. After inking, the stamp was brought into contact with the silicon wafer substrate; a very small amount of force was applied to make a good contact between both surfaces. The stamp was removed after 2 min, and the wafer was rinsed with PBS and deionized water and dried under nitrogen. The stamp could be used about 50 times without degradation of the printing capability when rinsed with water, water:ethanol mixture (80:20) and cleaned by sonication in ethanol (3 \times 10 min) after each inking and printing cycle.

The BSA-b micropattern produced by microcontact printing is presented schematically in Fig. 1(a). After microcontact printing of the BSA-b, the uncovered areas on the silicon substrate were blocked by immersing the wafer into a 2 mg ml⁻¹ BSA solution in PBS for 1 h [Fig. 1(b)] to avoid further nonspecific binding and/or sticking. After washing and drying, the wafer was incubated with a suspension of the avidin-coated Eu:Gd₂O₃ nanoparticles in carbonate-bicarbonate buffer for 1 h in a shaker to enable specific interaction between the avidin and biotin [Fig. 1(c)]. After the interaction took place, the substrate was rinsed with buffer and water, and dried under nitrogen before fluorescence and AFM studies.

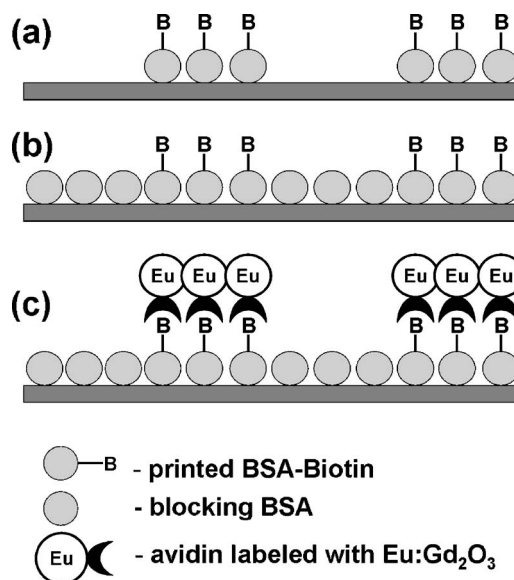


Fig. 1 Schematic description of microcontact printing of BSA-biotin (a), blocking with BSA (b), and specific interaction biotin with avidin-Eu:Gd₂O₃ (c).

3 Results and Discussion

3.1 Properties of the Eu:Gd₂O₃ Nanoparticles

The particle size distribution was determined by TEM analysis.¹¹ Most of the as-synthesized particles were nearly spherical with diameters between 5 and 500 nm. A narrower size distribution between 5 and 200 nm was obtained by means of selective centrifugation. Figure 2 represents a typical bright-field TEM micrograph of the sized nanoparticles. Three particles with sizes about 100 nm can be observed in the figure and one with a diameter of 15 nm. They have a dense morphology and approximately spherical shape.

The optical properties of the Eu:Gd₂O₃ nanoparticles were studied by using laser-induced luminescence. A colloidal solution of 1 mg ml⁻¹ in methanol was excited with a pulsed laser beam at a 260-nm wavelength. The slit width of the spectrophotometer was 0.8 nm. The luminescence emission spectrum in Fig. 3(a) shows an emission peak at 612 nm, which corresponds to the ⁵D₀→⁷F₂ electronic transition of

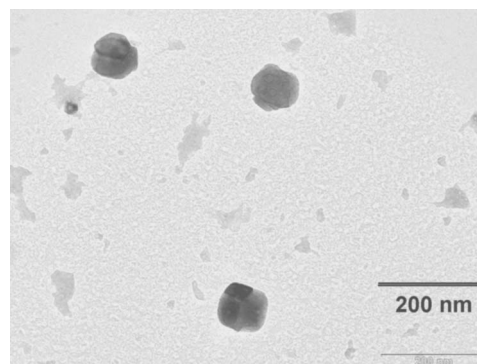


Fig. 2 Bright-field electron micrograph of Eu:Gd₂O₃ nanoparticles obtained by spray pyrolysis.

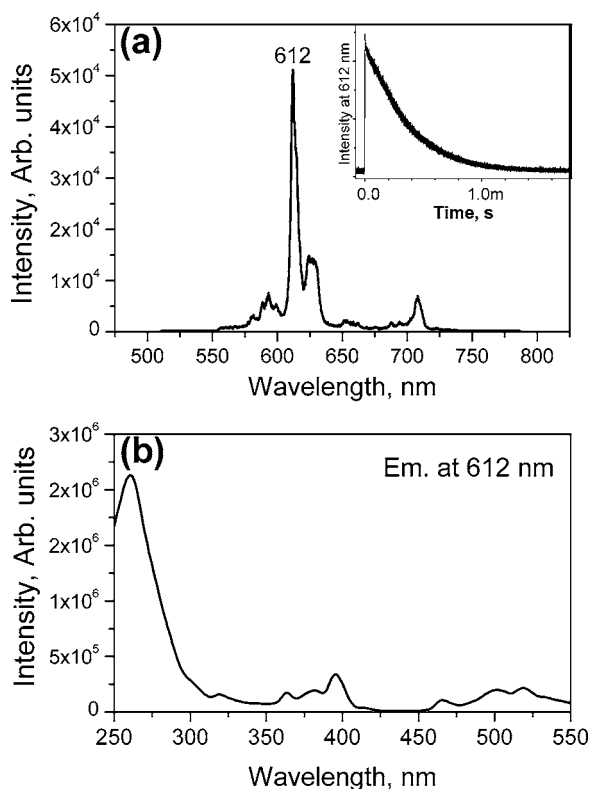


Fig. 3 (a) Luminescent emission spectrum of Eu:Gd₂O₃ nanoparticles (inset shows the luminescent lifetime) and (b) excitation spectrum of the Eu:Gd₂O₃ nanoparticles.

the Eu³⁺ ion in the Gd₂O₃ crystal lattice.³ The half-width of the peak is 5 nm, which is very narrow in comparison with other fluorophores. The excitation spectrum from Fig. 3(b) reveals multiple excitation peaks far from the emission at 612 nm. The most efficient excitation is in the UV range between 250 and 280 nm. Some additional excitation peaks are distributed in the range between 350 to 400 and 450 to 550 nm. This offers the possibility to choose between different excitation sources according to the experimental setup and the application.

In addition to the Eu doping into the Gd₂O₃ host, we performed doping with other lanthanide ions such as Tb, Dy, Sm, and Tm (data not shown). This is achieved by using the same synthesis process and changing the doping precursor [e.g., Tb(NO₃)₃ instead of Eu(NO₃)₃]. This enables us to synthesize a variety of gadolinium oxide particles with different luminescent spectra and identical morphology and surface properties.

The photostability of Eu:Gd₂O₃ nanoparticles was evaluated by subjecting a 1 mg ml⁻¹ colloidal solution to a 10-ns pulsed UV laser beam ($\lambda=260$ nm) with an energy of 30 μ J and frequency of 20 Hz. The luminescence intensity of the nanoparticles was measured after different irradiation times and was compared to the initial intensity. For comparison, the same experiment was performed with a colloidal solution of commercially available polystyrene nanoparticles (diameter 92 nm) doped with Eu chelates (Seradyn™), which have very good brightness and spectral properties that are nearly identical to the Eu:Gd₂O₃ nanoparticles. We measured the lumi-

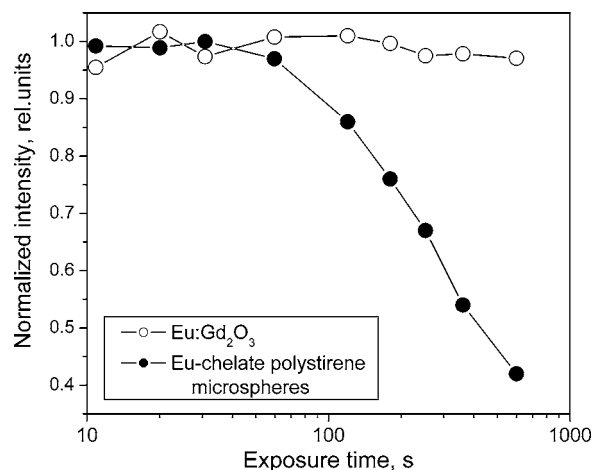


Fig. 4 Luminescence intensity change due to irradiation with UV laser ($\lambda=260$ nm) for Eu:Gd₂O₃ nanoparticles and polystyrene spheres impregnated with Eu chelates.

nescence intensity of the polystyrene nanoparticles to be about 10 times higher than that of Eu:Gd₂O₃ nanoparticles. Figure 4 shows a comparison of the relative luminescence intensity changes of the two samples after UV laser irradiation for up to 10 min. The intensity of Eu:Gd₂O₃ nanoparticles was not affected by the laser irradiation during the experiment. On the other hand, the polystyrene nanoparticles showed progressive photobleaching as the radiation was extended. Although the luminescence intensity of the chelate particles was not significantly affected after irradiation up to 1 min, it was reduced twofold after 6 min of irradiation and decreased by 40% of the initial value after 10 min of irradiation. Similar results regarding the bleaching of the same polystyrene particles were reported previously.¹³ Consecutive TEM studies showed that the size and shape of the polystyrene particles were not changed after the laser exposure. Therefore, we conclude that the Eu chelate complex was affected by the prolonged laser exposure.

The difference in the photostability between the polystyrene-chelate and the oxide particles was also visually observed on a fluorescent microscope, under excitation by a 100-W Hg lamp. The fluorescence of the polystyrene particles quickly decayed and the fluorescent image disappeared completely in less than 2 min. On the other hand, although oxide particles provided less bright images, the emission was stable for an effectively unlimited time of observation.

These results demonstrate one of the big advantages offered by the oxide particles—the high photostability, which makes them suitable for labels in a large variety of applications. In the case of microscopy applications, good photostability will provide enough time for image optimization and acquisition, while for quantitative measurements it will reduce the errors due to bleaching.

3.2 Coating of the Nanoparticles with Avidin

Because the avidin-biotin interaction has a high binding constant, this assay is widely used in molecular biology, immunoassay, diagnostics, and biosensor research. A demonstration using the avidin and biotin reaction system is the logical first step in an evaluation of a new format for biosensors, protein

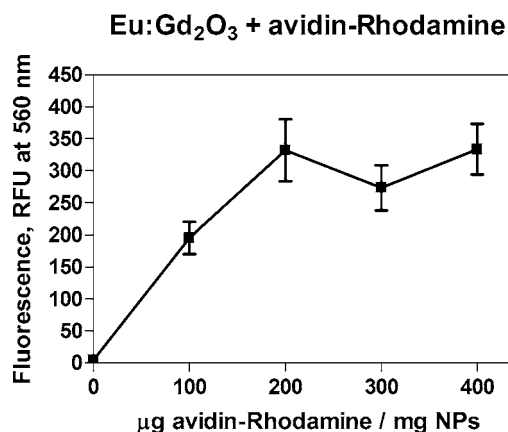


Fig. 5 Luminescent intensity of avidin-rhodamine adsorbed on 1-mg Eu:Gd₂O₃ nanoparticles, measured for different avidin-rhodamine coating concentrations.

chips, and other miniaturized analytical devices. Thus, we chose the avidin-biotin system as a model system in our studies to demonstrate the effectiveness of Eu:Gd₂O₃ nanoparticles as luminescent labels for micropattern imaging.

Avidin has been found to adsorb tightly to a variety of surfaces, such as dye-doped silica nanoparticles,¹⁴ carbon nanotubes,¹⁵ and quantum dots,^{12,16} due to electrostatic and/or hydrophobic interactions. Here, we take advantage of the negatively charged surface of the Eu:Gd₂O₃ nanoparticles to coat them with the avidin molecules using electrostatic interactions. The coating was carried out according to the experimental procedure already described. There are several advantages offered by this coating method: it is a one-step procedure (thereby avoiding chemical functionalization and conjugation steps); proteins retain their activity; conjugates are stable in a variety of buffers; the number of binding sites on the surface can be controlled by varying the coating concentration and they can be quantified easily; the nanoparticle's luminescence is not affected by the protein layer; and the nanoparticle surface can be efficiently blocked to avoid non-specific binding in immunoassays.

For evaluation of the avidin coating, Eu:Gd₂O₃ particles were coated with rhodamine-labeled avidin, following the procedure described in the experimental section. Using the measured fluorescence intensity of rhodamine, the amount of avidin that was adsorbed on the particle's surface was evaluated for different coating concentrations of avidin-rhodamine per 1 mg nanoparticles (Fig. 5). For concentrations up to 200 µg ml⁻¹, the amount of adsorbed avidin increased proportionally to the coating concentration, showing that the amounts of avidin were not enough to form dense monolayers on the particles' surfaces. For concentrations higher than 200 µg ml⁻¹, the adsorption of avidin did not depend on the coating concentration, indicating saturation of the particles' surfaces with avidin, suggesting the formation of a monolayer.

We estimated the formation of the adsorbed layer thickness on spherical nanoparticles by assuming a 100-nm average particle diameter and a 6×6-nm footprint of the avidin molecule.¹⁷ For 1 mg of particles with density 7.4 g cm⁻³ (for Gd₂O₃), the total surface area is 4×10⁻³ m². This surface can be covered by 3.2×10¹⁰ molecules (185 pmol) of avidin

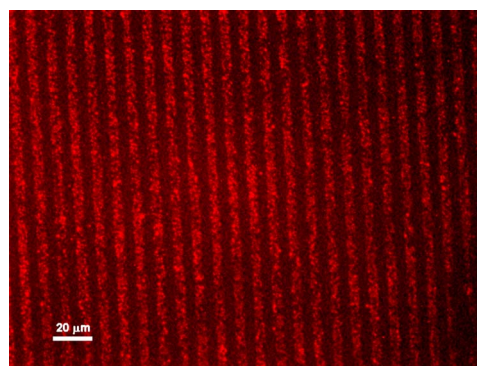


Fig. 6 Luminescence image of specifically immobilized avidin-Eu:Gd₂O₃ nanoparticles on printed BSA-biotin.

with a footprint area of 36 nm.² In other words, 185 pmol of avidin are necessary to form a densely packed monolayer on the surface of 1-mg nanoparticles in our case. This number is in excellent agreement with the experimentally obtained saturation level in Fig. 5, therefore supporting the assertion that a monolayer formed. Based on these results, we chose 200 µg of avidin per 1 mg of nanoparticles as coating concentrations for further experiments.

3.3 Fluorescence Imaging of BSA-Biotin Micropatterns with Avidin-Coated Eu:Gd₂O₃ Nanoparticles

The preparation of the BSA-biotin micropatterns and their interaction with the avidin coated Eu:Gd₂O₃ nanoparticles is schematically presented in Fig. 1 (see Sec. 2). The corresponding luminescent image is shown in Fig. 6. A series of alternating bright strips and dark strips can be observed. The actual width of the strips is 5 µm, which corresponds to the features of the PDMS stamp used for BSA-b printing. The bright strips correspond to the luminescent Eu:Gd₂O₃-avidin complexes that were specifically bound to the printed BSA-b. The dark strips, on the other hand, correspond to the blocked space between the printed strips where no avidin-coated particles were present. Although not all the bright strips had perfectly uniform fluorescent intensity, they were covered with specifically bound luminescent particles without large gaps. Densely packed bound particles showed up as higher intensity spots, while areas with lower surface density of bound particles were dimmer. On the other hand, very few particles could be observed in the BSA-passivated areas, demonstrating very low nonspecific binding in this case. The presence of clearly distinguishable fluorescent strips showed that the specific binding of avidin to biotin was not disturbed by the particles. In addition, the absence of particles between the strips confirmed that the blocking of the silicon substrate and the nanoparticles with BSA was sufficient to prevent non-specific binding of nanoparticles onto the substrate.

Another important conclusion is that the nonuniform size distribution of the nanoparticles may not disturb the specific binding and does not lead to nonspecific binding. This makes possible the use of polydispersed particles instead of expensive monodispersed particles. The lack of photobleaching of

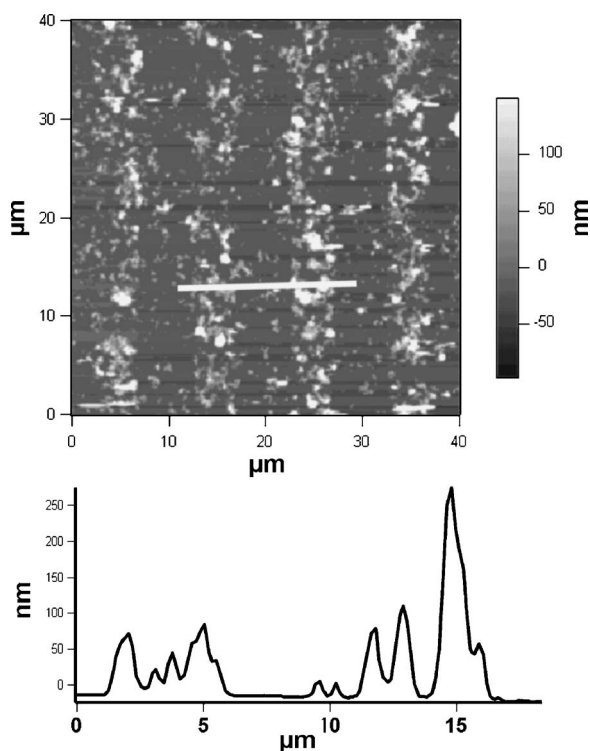


Fig. 7 AFM characterization of BSA-biotin micropatterns with avidin-Eu:Gd₂O₃ nanoparticles. Top: AFM topographic image of a micropatterned BSA-b after incubation with avidin-Eu:Gd₂O₃ particle for 1 h (image size is 40 × 40 μm²) and bottom: the cursor profile along the line in the top image shows that the height of the particles is in the range of 10 to 250 nm.

the Eu:Gd₂O₃ nanoparticles enabled the fluorescent image to be observed for an unlimited period of time facilitating image optimization.

3.4 AFM Characterization of BSA-Biotin Micropatterns with Avidin-Coated Eu:Gd₂O₃ Nanoparticles

We employed an AFM to image the immobilized avidin-Eu:Gd₂O₃ on a single particle level. The presence of solid nanoparticle labels with sizes larger than those of proteins on the substrate surface made it possible to evaluate the density of specifically and nonspecifically bound particles. An AFM topographic image of a randomly chosen region with a scan size of 40 × 40 μm² of the substrate is shown in top part of Fig. 7. Four vertical bright strips were visualized within the scan area as shown in Fig. 7. The surface density of specifically bound particles on the strips was much higher than the density of nonspecifically bound particles shown as scattered bright spots between the line patterns. The selectivity achieved here is the basis for applying this approach as a detection technique.

The nonspecific binding of particles could be minimized possibly by further optimization of the coating and washing processes. We believe that the nonuniform density of the specifically bound particles could be partially due to reduced diffusion near the substrate surface and partially due to formation of small aggregates of particles during the incubation. This effect could be avoided by optimization of the incubation

protocols. A cursor profile, which was taken along the white line in the AFM image, is shown in the bottom part of Fig. 7. According to the cursor profile, the particles on the strips have heights between about 10 and 250 nm. The majority of the particles exhibit heights between 50 and 100 nm. This height measurement is consistent with the particle size known from TEM studies. It is clear that these particles are the immobilized avidin-coated nanoparticles. The spatial resolution and the uniformity of protein micropattern visualization could be improved by using smaller, nearly monodispersed particles.

4 Conclusions

This is the first demonstration that luminescent nanoparticles made of lanthanide oxides can be successfully used for visualizing protein micropatterns. The unique spectral properties, good photostability, and low price of the synthesis of these novel materials offer an attractive alternative to other widely used fluorophores. The surface properties of the Eu:Gd₂O₃ nanoparticles presented in this paper enable easy one-step biofunctionalization of the particles. The avidin coating of Eu:Gd₂O₃ nanoparticles can be used as a base shell for the preparation of nanoparticle conjugates with a variety of biotin-modified antibodies recognizing the desired target. The coating procedure can be directly transferred to lanthanide oxides with different spectral properties (e.g., Tb:Gd₂O₃, Dy:Gd₂O₃, Sm:Gd₂O₃, etc.) enabling multilabel/multianalyte detection. Those conjugates can be applied to the optical detection of a variety of molecules in an array format, e.g., for microimmunoassays and for DNA arrays.

Acknowledgments

The authors wish to acknowledge the assistance of Professor Y. Xia of the University of Washington for providing the PDMS stamp used in this work, and the support of the National Science Foundation, Grant No. DBI-0102662 and the Superfund Basic Research Program with Grant No. 5P42ES04699 from the National Institute of Environmental Health Sciences, National Institute of Health (NIH).

References

1. R. N. Bhargava, "Doped nanocrystalline materials—physics and applications," *J. Lumin.* **70**, 85–94 (1996).
2. B. M. Tissue, "Synthesis and luminescence of lanthanide ions in nanoscale insulating hosts," *Chem. Mater.* **10**, 2837–2845 (1998).
3. W. O. Gordon, J. A. Carter, and B. M. Tissue, "Long-lifetime luminescence of lanthanide-doped gadolinium oxide nanoparticles for immunoassays," *J. Lumin.* **108**, 339–342 (2004).
4. C. B. Murray, D. J. Norris, and M. G. Bawendi, "Synthesis and characterization of nearly monodisperse CdE (E=S, Se, Te) semiconductor nanocrystallites," *J. Am. Chem. Soc.* **115**, 8706–8715 (1993).
5. M. Bruchez, M. Moronne, P. Gin, S. Weiss, and A. P. Alivisatos, "Semiconductor nanocrystals as fluorescent biological labels," *Science* **281**, 2013–2016 (1998).
6. W. C. W. Chan and S. M. Nie, "Quantum dot bioconjugates for ultrasensitive nonisotopic detection," *Science* **281**, 2016–2018 (1998).
7. I. L. Medintz, H. T. Uyeda, E. R. Goldman, and H. Mattoussi, "Quantum dot bioconjugates for imaging, labelling and sensing," *Nat. Mater.* **4**, 435–446 (2005).
8. J. Feng, G. M. Shan, A. Maquieira, M. E. Koivunen, B. Guo, B. D. Hammock, and I. M. Kennedy, "Functionalized europium oxide nanoparticles used as a fluorescent label in an immunoassay for atrazine," *Anal. Chem.* **75**, 5282–5286 (2003).
9. A. Bernard, J. P. Renault, B. Michel, H. R. Bosshard, and E. Delamarche, "Microcontact printing of proteins," *Adv. Mater. (Wein-*

- heim, Ger.*) **12**, 1067–1070 (2000).
10. "Amine-reactive Probes," <http://www.probes.com>.
 11. D. Dosev, B. Guo, and I. M. Kennedy, "Photoluminescence of Eu³⁺:Y₂O₃ as an indication of crystal structure and particle size in nanoparticles synthesized by flame spray pyrolysis" *J. Aerosol Sci.* (in press).
 12. E. R. Goldman, E. D. Balighian, H. Mattoussi, M. K. Kuno, J. M. Mauro, P. T. Tran, and G. P. Anderson, "Avidin: a natural bridge for quantum dot-antibody conjugates," *J. Am. Chem. Soc.* **124**, 6378–6382 (2002).
 13. V. Vaisanen, H. Harma, H. Lilja, and A. Bjartell, "Time-resolved fluorescence imaging for quantitative histochemistry using lanthanide chelates in nanoparticles and conjugated to monoclonal antibodies," *Luminescence* **15**, 389–397 (2000).
 14. R. Tapeç, X. J. J. Zhao, and W. H. Tan, "Development of organic dye-doped silica nanoparticles for bioanalysis and biosensors," *J. Nanosci. Nanotechnol.* **2**, 405–409 (2002).
 15. F. Balavoine, P. Schultz, C. Richard, V. Mallouh, T. W. Ebbesen, and C. Mioskowski, "Helical crystallization of proteins on carbon nanotubes: a first step towards the development of new biosensors," *Angew. Chem., Int. Ed.* **38**, 1912–1915 (1999).
 16. H. Mattoussi, J. M. Mauro, E. R. Goldman, G. P. Anderson, V. C. Sundar, F. V. Mikulec, and M. G. Bawendi, "Self-assembly of CdSe-ZnS quantum dot bioconjugates using an engineered recombinant protein," *J. Am. Chem. Soc.* **122**, 12142–12150 (2000).
 17. W. A. Hendrickson, A. Pahler, J. L. Smith, Y. Satow, E. A. Merritt, and R. P. Phizacker, *Proc. Natl. Acad. Sci. U.S.A.* **86**, 2190–2194 (1989).